

Marked Effects of Alloying on the Thermal Conductivity of Nanoporous Materials

Chandan Bera,^{1,2} Natalio Mingo,^{1,*} and Sebastian Volz²

¹CEA, LITEN, 17 rue des Martyrs, 38054 Grenoble, France

²Laboratoire d'Énergie Moléculaire et Macroscopique, CNRS UPR 288, Ecole Centrale Paris, France

(Received 15 June 2009; revised manuscript received 15 January 2010; published 18 March 2010)

We show that porous alloys can display thermal conductivity reductions at considerably larger pore sizes than nonalloyed porous materials of the same nominal porosity. The thermal conductivity of $\text{Si}_{0.5}\text{Ge}_{0.5}$ alloy with 0.1 porosity becomes half the nonporous value at 1000 nm pore sizes, whereas pores smaller than 100 nm are required to achieve the same relative reduction in pure Si or Ge. Using Monte Carlo simulations, we also show that previous models had overestimated the thermal conductivity in the small pore limit. Our results imply that nanoporous alloys should be advantageous with respect to nanoporous nonalloys, for applications requiring a low thermal conductivity, such as novel thermoelectrics.

DOI: 10.1103/PhysRevLett.104.115502

PACS numbers: 63.22.-m, 44.30.+v, 65.80.-g, 66.70.-f

There is common consensus that important thermal conductivity reductions should be expected in nanoporous materials, as the diameter and distance between the nanopores are made smaller [1–4]. However, concrete trends beyond this qualitative assessment are not yet clearly understood. In fact, we will show here that some of the dependencies previously predicted stem from oversimplifications in the model used, rather than from the real physical behavior of the system. Also, most previous efforts have concentrated on the thermal conductivity of nanoporous nonalloy matrices, such as pure Si. Previous works addressing SiGe considered nanocomposites comprising individual nanosized parts of pure Si and pure Ge, but they did not address the case where the matrix is a random alloy at the atomic level [5]. Here we show that the thermal conductivity of nanoporous alloys behaves in a qualitatively different way than that of nonalloys, and this may be very advantageous for certain applications.

We have focused on the thermal conductivity of parallel pore arrangements, in the direction parallel to the pores. To investigate these systems, a cylindrical geometry approximation (CGA) was proposed in Ref. [3], where the thermal conductivity was found by numerical solution of the frequency independent Boltzmann transport equation. In parallel, the CGA was also employed in Ref. [2], which provided the exact analytical solution to the Boltzmann equation for this geometry. An extension of this analytical calculation to the frequency dependent case was given in Ref. [6]. The CGA consists in replacing the porous medium by a single pore surrounded by a specularly reflecting cylindrical boundary [2,3]. This in principle should mimic the fact that when a phonon gets away from the pore, it will approach a different pore nearby. The other boundary condition, at the surface of the pore, can be chosen to be partly or totally diffusive.

The results presented in Refs. [2,3] numerically agree with each other, as they should. However, the CGA employed there leads to the peculiar result that, for fixed pore

volume fraction (or porosity), the thermal conductivity does not decrease indefinitely upon pore size reduction, but saturates below a certain pore size. The reason why this occurs is implicit in the analytical solution [2], which shows the presence of a continuous range of phonon directions that keep circling around the system without ever colliding with the pore [see Fig. 1(a)]. This finite fraction of phonons gives a contribution equal to the bulk thermal conductivity weighted by the fraction of angles in which the infinite circling occurs, $F = 1 - \frac{2 \arcsin(\sqrt{\epsilon})}{\pi}$, where ϵ is the porosity. So the saturated thermal conductivity for infinitely small, infinitely close pores, is given by $\kappa = (1 - \epsilon)F\kappa_{\text{bulk}}$. Obviously, this result is linked to the model, and the question is whether the predicted saturation has any physical meaning. Intuitively, it is apparent that the real pore configuration will not show any continuous range of angles that do not intersect a pore: sooner or later, a line in

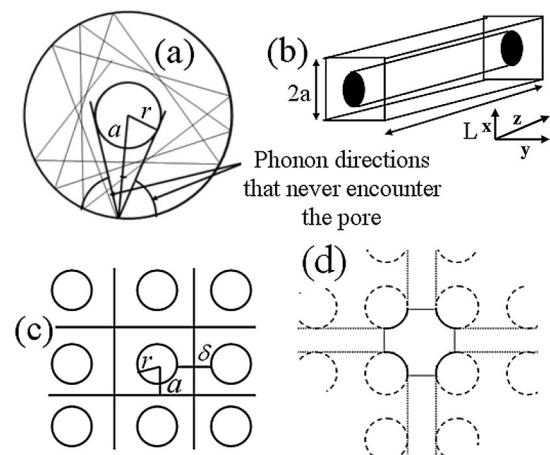


FIG. 1. (a) A drawback of the CGA: in the small pore radius limit some phonons never collide with the pore. (b) Square arrangement geometry used for the three dimensional Monte Carlo calculation. (c) Top view of the nanopore array. (d) Geometry used for the analytical interpolation Eq. (2).

any chosen direction should hit a pore. (This excludes high symmetry directions, if one considers ordered arrangements; but even then, the range of “unblocked” angles is not continuous, in contrast with the CGA.) Thus, the answer to whether a saturation should occur is not obvious, and the way the thermal conductivity might depart from the CGA prediction is *a priori* unclear.

To answer these questions we have implemented a Monte Carlo (MC) simulation of phonon transport through a three dimensional array of parallel pores. The pores are organized in a square mesh configuration Fig. 1(c). This allows us to reduce the simulation to a cell containing one pore, with periodic boundary conditions in the (x, y) directions [Fig. 1(b)] [7]; the system is bounded between two perfectly absorbing phonon blackbody reservoirs in the z direction.

First, we have investigated how much the mean free paths Λ are affected due to the presence of the pores. Λ is computed as a function of the bulk mean free path Λ_0 , the pore radius r , and the porosity ϵ . The interpore distance, δ , is related to the pore radius and porosity as $\delta = 2r((0.5/\sqrt{\epsilon}) - 1)$. An additional variable is the length of the system, L [Fig. 1(b)], which needs to be taken in the long length limit.

To obtain the effective mean free path, one launches a large number N of particles (phonons) from one end of the system ($z = 0$), and lets them evolve until they come out through either side ($z = L$ or $z = 0$). Phonons are injected at $z = 0$ with a random initial direction and random initial position in the x, y plane within the primitive mesh. The fraction of particles that transmit across the whole length, N_{through} , reaches a diffusive type dependence with length for sufficiently long systems, given by

$$N_{\text{through}}/N \simeq (1 + L/\Lambda)^{-1}. \quad (1)$$

We perform the simulation enlarging L until the above behavior is attained with enough precision. The mean free path is then evaluated from the slope of the inverse throughput fraction, using Eq. (1).

The phonon trajectories are described by a MC technique [8]. A random direction and a free path s are generated after each scattering event. s is obtained as $s = -\ln R_s \times \Lambda_0$, where R_s is a random number between 0 and 1. It can be verified that this model is equivalent to other descriptions based on time steps discretization [9,10], and that it yields the correct solution to the diffusion equation. The simulations employed 10^6 phonons, which ensures satisfying statistical averages. L was increased until a good accuracy was obtained ($\geq 99\%$).

In order to verify that this method accurately yields the mean free paths, we have first applied it to reproduce the CGA results given analytically in Ref. [2]. As shown in Fig. 2(a), the numerical MC results (open symbols) are in very good agreement with the exact analytical results (red lines). This makes us confident that our computations for the fully 3D square geometry are also accurate.

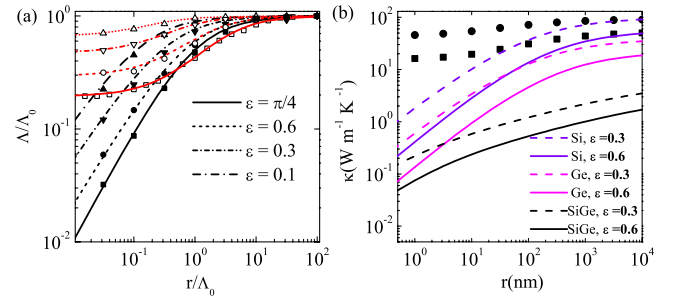


FIG. 2 (color online). (a) Dimensionless mean free path for $\epsilon = 0.1, 0.3, 0.6$, and $\frac{\pi}{4}$, calculated by: MC CGA approximation (open symbols), analytical CGA (red lines), MC fully 3D (closed symbols), and Eq. (3) (black lines). (b) Conductivity of Si, Ge, and Si_{0.5}Ge_{0.5} at 30% and 60% porosity. The symbols correspond to the CGA result for Si with $\epsilon = 0.3$ (circles) and $\epsilon = 0.6$ (squares).

The shortening of the mean free path with pore size for the real systems is shown as closed symbols in Fig. 2(a). The figure shows that when the intrinsic bulk mean free path Λ_0 is larger than the pore size and interpore separation, the size effect becomes important. However, contrary to the CGA’s prediction (red lines), no saturation occurs at small pore size. The mean free path keeps decreasing indefinitely as the pores become smaller. It is tempting to associate the decrease with a formula of the Casimir type, in which the role of the system’s size would be played by the interpore separation d , as $\Lambda \sim d$ [11]. However, the log-log plot in Fig. 2(a) shows that this oversimplified form does not match the results, except when the volume fraction exceeds $\frac{\pi}{4}$. When $\epsilon > \frac{\pi}{4}$ the nanopores touch each other, so that the system becomes an array of parallel independent nanowires, which is well described by $\Lambda \sim d$ [12]. However, for $\epsilon < \frac{\pi}{4}$ the system becomes connected, and the thermal conductivity depends on d more slowly.

We can understand this behavior as follows. Within the unit mesh depicted in Fig. 1(d), we have a fraction of the boundary $C = 1/(1 + 2\delta/\pi r)$ (thick solid line) that is covered by the pores. The remaining fraction, $1 - C$ (thin solid lines), is open and it allows the particles to traverse into a neighboring mesh. Most of the phonons that traverse to a neighboring mesh via the opening between pores, will do so in a rather shallow angle. This means that the effective row of pores seen by those phonons looks more like two continuous parallel plates [dotted lines in Fig. 1(d)]. One can therefore try to interpolate the total mean free path as a simple combination of the Casimir type mean free path for a wire of radius r [11], $\Lambda_{\text{casimir}}(\omega) = (1/\Lambda_0(\omega) + 1/(2Br))^{-1}$, and the mean free path for a thin film given by Lucas [13], $\Lambda_{\text{Lucas}}(\omega, D) = \Lambda_0(\omega)(1 - \frac{3\Lambda_0(\omega)}{4D} \int_0^1 2(x - x^3)(1 - e^{-D/x\Lambda_0(\omega)})dx)$. B is a parameter associated to the shape of the wire’s cross section, and D is the thickness of the equivalent film. Therefore, a plausible form is

$$\Lambda(\omega) \simeq C\Lambda_{\text{casimir}}(\omega) + (1 - C)\Lambda_{\text{Lucas}}(\omega, A \times r/\sqrt{\epsilon}), \quad (2)$$

where $A \equiv D\sqrt{\epsilon}/r$ is the only adjustable parameter. B should not be considered adjustable; rather, it corresponds to the case of $\epsilon = \frac{\pi}{4}$, when the system becomes a nanowire array, with $B = 0.85$.

The proposed formula works remarkably well. Figure 2(a) shows a comparison between the MC (closed symbols) and analytical (black lines) results for a large range of porosities and pore sizes. The best fit was obtained for $A = 1.85$. This formula is extremely practical, because it allows for a very fast computation of the effective mean free paths (MFP) of the nanoporous material, for any values of Λ_0 , r , and ϵ , with good accuracy. This is advantageous in the application of these results to compute the thermal conductivity of concrete nanoporous materials, detailed below.

In the relaxation time approximation, the thermal conductivity can be expressed as an integral over frequencies of the form [Eq (10) of Ref. [12]]

$$\kappa = \int_0^{xc} \frac{df_B}{dT} \Lambda(\omega) \mathcal{T}_0(\omega) \hbar \omega d\omega / 2\pi, \quad (3)$$

where $\mathcal{T}_0(\omega) = \frac{1}{2} \sum_{\alpha=1}^6 \int_{BZ} \delta(\omega - \omega_{\alpha}(\vec{q})) \left| \frac{d\omega_{\alpha}(\vec{q})}{dq_x} \right| d\vec{q} / 2\pi$, $\Lambda(\omega)$ is the total mean free path, and f_B is the Bose distribution. The thermal conductivity of the nanoporous material is therefore given by the equation above, using the mean free paths computed via the MC simulation, $\Lambda(\omega) = \Lambda_{MC}(\Lambda_0(\omega), \delta, r)$, where $\Lambda_0(\omega)$ is the bulk MFP of the matrix material. The phonon dispersion relations for Si and Ge were obtained via the Harrison interatomic potential [12,14]. The phonon dispersion for SiGe was considered in the standard virtual crystal approximation, by averaging the force constants of Si and Ge. The bulk MFP's $\Lambda_0(\omega)$ for Si and Ge were computed in the way explained in Ref. [12], and they yield a good match to the bulk crystal thermal conductivity in the 50–900 K temperature range. The bulk MFP for the alloy includes the additional *alloy scattering term* [15,16]. We verified that the experimental bulk alloy thermal conductivity [15] is well reproduced up to temperatures of 900 K. Using the interpolation expression, Eq. (2), combined with the knowledge of $\Lambda_0(\omega)$ allows us to efficiently compute κ . In addition to the full dispersions approach just described, we also tried the non-dispersive model introduced at the end of Ref. [12] [see Eq. (15) in this reference, and also Refs. [16,17]], obtaining results very close to the ones yielded by the full dispersions model.

The computed room temperature thermal conductivities of nanoporous Si, Ge, and $\text{Si}_{0.5}\text{Ge}_{0.5}$ are shown in Fig. 2(b) as a function of pore radius, for various porosities. For comparison, results using the CGA mean free paths are also plotted for the Si case (filled symbols). The differences become very large as the pore radius becomes small enough to visibly affect the mean free path. This graph shows that the CGA yields a quite inaccurate representation of the phonon MFP and κ of the nanoporous system.

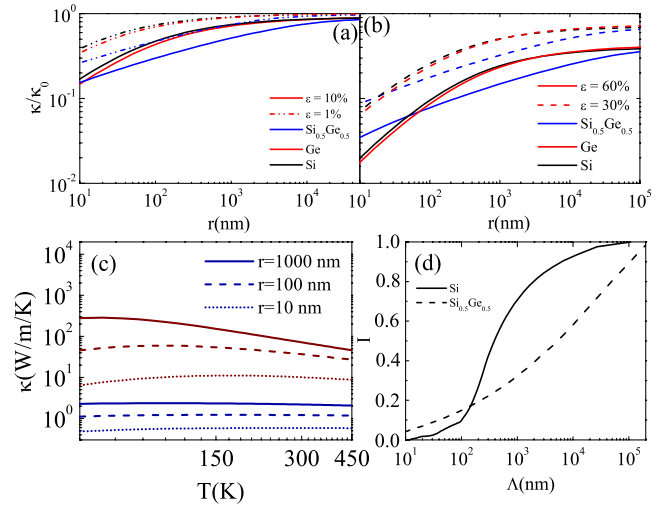


FIG. 3 (color online). (a) Thermal conductivity of Si, Ge, and $\text{Si}_{0.5}\text{Ge}_{0.5}$ at 1% and 10% porosity, normalized by their bulk values. (b) Thermal conductivity of Si and $\text{Si}_{0.5}\text{Ge}_{0.5}$ at 30% and 60% porosity, normalized by their bulk values. (c) $\kappa(T)$ for different pore sizes, for Si and $\text{Si}_{0.5}\text{Ge}_{0.5}$ at 30% porosity. (d) Relative contribution $I(\Lambda)$ to the thermal conductivity associated to phonons with MFP's shorter than Λ , plotted as a function of $\Lambda(\omega)$, for bulk Si and $\text{Si}_{0.5}\text{Ge}_{0.5}$ at room temperature. ($I \rightarrow 1$ in the limit $\Lambda \rightarrow \infty$.)

An even more striking finding is the noticeably different behavior of the alloy and nonalloy material thermal conductivities as a function of pore size. This is clear on the plot of the porous material conductivity normalized by the bulk material conductivity, in Fig. 3. The alloy material is considerably affected by the presence of a 10% porosity already at pore sizes of 1000 nm, whereas the pure Si and Ge cases are barely affected at this pore size. Only below 100 nm pore size do the 10% porosity pure Si and Ge matrices start displaying a size effect. These pore sizes become about 5 times bigger for porosities close to the nanowire limit ($\epsilon = \pi/4$). The room temperature thermal conductivity of bulk $\text{Si}_{0.5}\text{Ge}_{0.5}$ is just 1 order of magnitude smaller than those of Si or Ge, but this difference becomes 2 orders of magnitude when comparing nanoporous materials with $r \sim 200$ nm at 10% porosity, or with $r \sim 1000$ nm at 60% porosity. Below this diameter, the decrease becomes faster in the nonalloys. Nonetheless, the absolute thermal conductivity of SiGe always stays smaller than that of Si or Ge for the same porosity and size, as one would expect.

The reason for the pore effect being noticeable in the alloy at considerably larger pore diameters than in the nonalloy case, is related to the very sharp dependence of the alloy scattering mean free path. Alloys have a reduced thermal conductivity well below that of their individual components, because atomic scale disorder can scatter short wavelength phonons very efficiently. Longer wavelength phonons, however, can have mean free paths many orders of magnitude larger than the short wavelength ones. For nonalloys, the contrast between long and short wave-

length mean free paths is not so marked, and a considerable amount of heat is carried by the short wavelengths. Introducing nanopores affects the long wavelengths more strongly than the short ones. This is because the former have longer mean free paths than the latter, and according to Fig. 2(a), the effect of the pores becomes noticeable when their separation starts to be comparable to the bulk mean free path. Since heat in the alloys is carried by a very small range of phonon frequencies, with very long mean free paths, rather large pores are already able to block a large fraction of that heat. For nonalloys, heat is carried in a larger frequency range, so even if the pores can block the long MFP phonons, there is a non-negligible amount of shorter MFP phonons which still requires smaller pores in order to be affected. (A similar behavior has been identified in the case of nanodots embedded into a matrix [16].)

For each value of the mean free path Λ , Fig. 3(d) shows the contribution to the bulk thermal conductivity of all phonons having $\text{MFP} < \Lambda$. For SiGe most of the heat is carried by phonons with $\text{MFP} > 10 \mu\text{m}$. In contrast, in Si a significant fraction of the heat is carried by phonons with shorter intrinsic MFP, which are less affected by the pores. Figure 3(a) shows κ/κ_0 for a small porosity of 1%. For large pores the macropore limit $1 - \epsilon$ is retrieved. Size effects are more appreciable for SiGe than for Si, consistently with our previous discussion.

It is experimentally known that phonon scattering with pores or cavities can mask interphonon scattering, thus rendering the effective thermal conductivity nearly independent of temperature [18,19]. Our calculation also yields this effect, as shown in Fig. 3(c). As expected, the effect is more pronounced for smaller pore sizes. SiGe is more strongly affected than Si at comparable pore sizes, for the reasons explained in the previous paragraph.

The remarkable differences just described between the thermal conductivities of alloy and nonalloy nanoporous materials imply that nanoporous alloys may be very advantageous for certain applications. For example, nanoporous materials have been proposed as potentially interesting thermoelectrics [6,20]. Difficulty to produce nanosized pores may however be an obstacle for their synthesis. Furthermore, the pore surfaces might in some cases act as charge traps and considerably decrease electron mobility [21]. Using a porous alloy instead would allow us to take advantage of the thermal conductivity reduction at much larger pore sizes. Thus, they would be easier to synthesize, and additionally their surface to volume ratio would be smaller than in the nonalloy case, minimizing the problem of electron scattering by surface charges.

In sum, via a MC simulation we have accurately evaluated the phonon MFP's of parallel nanoporous materials. We have found that a previously used cylindrical geometry approximation yields an inadequate description of the actual mean free paths in the real system. The behavior of the MFP with pore size and porosity can be understood as a combination of a wire and film behavior, and a suitable interpolation formula has been provided that accounts well

for all the MC results. For small pores, calculation of the thermal conductivity using the correct MFP's yields results considerably lower than those predicted in earlier publications. We have then investigated the thermal conductivity of porous Si, porous Ge, and porous SiGe alloy, obtaining an important qualitative difference between the alloy and the nonalloys. The thermal conductivity of the alloy is strongly affected by pores even at large ($1 \mu\text{m}$) diameters. In contrast, the thermal conductivity of Si or Ge is only affected when the pores are considerably smaller ($< 100 \text{ nm}$), due to the rather different competing phonon scattering mechanisms acting in alloys and nonalloys. These remarkable differences are highly relevant for applications targeting thermal conductivity reduction, such as nanostructured thermoelectric materials, where we have shown that the use of an alloy is potentially advantageous.

We thank M. Plissonnier for discussions and advise. C.B. acknowledges financial support from CEA. N.M. thanks R.A. Prasher for helpful discussions. Work supported by project Thermaescape, ANR-06-NANO-054-01.

*Corresponding author.
natalio.mingo@cea.fr

- [1] J. D. Chung and M. Kaviany, *Int. J. Heat Mass Transf.* **43**, 521 (2000).
- [2] R. Prasher, *J. Appl. Phys.* **100**, 034307 (2006).
- [3] R. Yang, G. Chen, and M. S. Dresselhaus, *Phys. Rev. B* **72**, 125418 (2005).
- [4] J.-H. Lee, J. C. Grossman, J. Reed, and G. Galli, *Appl. Phys. Lett.* **91**, 223110 (2007).
- [5] R. Yang and G. Chen, *Phys. Rev. B* **69**, 195316 (2004).
- [6] N. Mingo and D. A. Broido, *J. Appl. Phys.* **101**, 014322 (2007).
- [7] It might also be possible to obtain an analytical solution to the BTE in this geometry, alternatively to the MC simulation [R. Prasher (private communication).]
- [8] *Microscale and Nanoscale Heat Transfer*, edited by S. Volz (Springer, Paris, 2005), p. 33.
- [9] S. Mazumder and A. Majumdar, *J. Heat Transfer* **123**, 749 (2001).
- [10] D. Lacroix, K. Joulain, and D. Lemonnier, *Phys. Rev. B* **72**, 064305 (2005).
- [11] J. M. Ziman, *Electrons and Phonons* (Clarendon Press, Oxford, 2001).
- [12] N. Mingo, *Phys. Rev. B* **68**, 113308 (2003).
- [13] M. S. P. Lucas, *J. Appl. Phys.* **36**, 1632 (1965).
- [14] N. Mingo and L. Yang, *Phys. Rev. B* **68**, 245406 (2003).
- [15] B. Abeles, *Phys. Rev.* **131**, 1906 (1963).
- [16] N. Mingo, D. Hauser, N. P. Kobayashi, M. Plissonnier, and A. Shakouri, *Nano Lett.* **9**, 711 (2009).
- [17] N. Mingo *et al.*, *Nano Lett.* **3**, 1713 (2003).
- [18] N. Savvides and H. J. Goldsmid, *J. Phys. C* **13**, 4657 (1980).
- [19] D. Song and G. Chen, *Appl. Phys. Lett.* **84**, 687 (2004).
- [20] D. A. Broido and N. Mingo, *Phys. Rev. B* **74**, 195325 (2006).
- [21] M. Ben Chorin, F. Moller, and F. Koch, *Phys. Rev. B* **49**, 2981 (1994).